

Detecting Scalar Higgs Bosons in the Next-to-Minimal Supersymmetric Standard Model at Future Linear Colliders

B. R. Kim* and G. Kreyerhoff

III. Phys. Inst. A, Physikzentrum, RWTH Aachen
Aachen, 52056, Germany

S. K. Oh

Department of Physics, Kon-Kuk University
Seoul 143-701, Korea

Abstract

We analyze the possibility of detecting one of the three scalar Higgs bosons in the next-to-minimal supersymmetric model at the future e^+e^- linear collider, by examining their productions via the Higgsstrahlung process. The production cross sections of the three scalar Higgs bosons in e^+e^- collisions are evaluated for the proposed c.m. energies of the future e^+e^- colliders, for the whole space of relevant parameters. We find that at least one of the three production cross sections is not smaller than 16 fb, 4 fb, and 1 fb for $\sqrt{s} = 500$ GeV, 1000 GeV, and 2000 GeV, respectively. Those numbers indicate that at least one of the three scalar Higgs bosons in the next-to-minimal supersymmetric model may be detected at the future e^+e^- linear colliders via the Higgsstrahlung process.

*E-mail: kim@physik.rwth-aachen.de (telephone +49-241-80-7239)

The scalar Higgs bosons constitute an essential part of the standard model and the extended models therefrom [1]. To search for and discover them is thus one of the most important tasks of both theoretical and experimental particle physicists. As is well known, there is just one scalar Higgs boson, S , in the standard model, whereas there are multiples of them in the extended models. For example, the minimal supersymmetric standard model (MSSM) [2] has two scalar Higgs bosons, S_1 and S_2 , while the next-to-minimal supersymmetric standard model (NMSSM) [3] has three of them: S_1 , S_2 , and S_3 .

The MSSM has just two gauge doublet Higgs superfields, \mathcal{H}_1 and \mathcal{H}_2 , and the NMSSM is a minimal extension of the MSSM, by introducing an additional gauge singlet Higgs superfield $\mathcal{N} = (N, \psi_N, F_N)$ to the Higgs sector of the MSSM. Here, N is a Higgs singlet, ψ_N is a singlet higgsino, and F_N is an auxiliary field. As mentioned elsewhere [4], this singlet superfield can provide an economical way to avoid the so called μ -parameter problem in the MSSM. Thus, while the MSSM introduces the dimensional μ -parameter by hand, the NMSSM can generate it in terms of the singlet superfield \mathcal{N} .

In the NMSSM, the relevant superpotential is given by

$$\mathcal{W} = \lambda \mathcal{H}_1^T \epsilon \mathcal{H}_2 \mathcal{N} - \frac{1}{3} k \mathcal{N}^3 + \dots \quad (1)$$

where λ and k are dimensionless parameters. We assume that they are real. The relevant soft-breaking part of the Higgs sector is accordingly given by

$$V_{\text{soft}} = -\lambda A_\lambda H_1^T \epsilon H_2 N - \frac{1}{3} k A_k N^3 + \text{h.c.} + \dots \quad (2)$$

where A_λ and A_k are soft-breaking parameters having mass dimension. As the vacuum expectation value $\langle N \rangle_0 = x$ is developed, λx emerges to correspond to the μ -parameter in the MSSM superpotential $\mathcal{W} = \mu \mathcal{H}_1^T \epsilon \mathcal{H}_2 + \dots$. Note that the Peccei-Quinn symmetry is recovered if $k = 0$. Thus, $\lambda k \neq 0$. The two Higgs doublets H_1 and H_2 give masses to the up-quark sector and the down-quark sector, when they develop the vacuum expectation values, v_1 and v_2 , respectively.

A side effect of the introduction of the new superfield is that it enriches the particle spectra of the NMSSM as well as introduces more parameters than the MSSM. While the charged sector of the NMSSM is the same as that of the MSSM, the neutral sector of the NMSSM has an extra neutralino, an extra scalar Higgs and an extra pseudoscalar Higgs boson. The number of parameters in the NMSSM is also larger than in the MSSM. For example, while one needs just two parameters in order to determine the Higgs boson masses in the MSSM, which can be chosen as μ and $\tan \beta = v_1/v_2$, six parameters are introduced for the same purpose in the NMSSM: λ , x , k , A_λ , A_k , and $\tan \beta$.

The present experiments at LEP set lower bounds on the mass of the lightest scalar Higgs boson. The standard scalar Higgs boson may not be lighter than 65

GeV, while S_1 in the MSSM may not have a mass below 45 GeV as it has not been detected yet [5]. For the scalar Higgs bosons in the NMSSM, it is shown that there are parameter regions where the lightest scalar Higgs boson S_1 may have a small mass without contradicting to the present experimental data [6].

Our main purpose in this article is to show that at least one of the scalar Higgs bosons in the NMSSM can be detected at the future e^+e^- Linear Colliders with $\sqrt{s} = 500, 1000, \text{ or } 2000$ GeV. This is done by calculating the minima of the production cross sections of the three scalar Higgs bosons in e^+e^- collisions. We find that there are parameter regions in the NMSSM where at least one of the minima of the production cross sections are larger than the proposed discovery limit of the future e^+e^- colliders, which implies that the future e^+e^- colliders are capable of detecting at least one of the three scalar Higgs bosons in the NMSSM. A preliminary result of our analysis is reported elsewhere [7].

A remarkable result of the MSSM is that there is an upper bound on the mass of the lighter scalar Higgs boson given by

$$m_{S_1} \leq m_Z \cos 2\beta$$

at the tree level. This is due to the fact that all quartic terms have gauge coupling constants. In case of the NMSSM with one Higgs singlet, there are quartic terms with couplings other than the gauge couplings. Thus, there is no simple upper bound on the mass of scalar Higgs boson as in the MSSM. The tree-level upper bound on m_{S_1} is given as [8]

$$m_{S_1}^2 \leq (m_{S_1}^{\max})^2 = m_Z^2 \left(\cos^2 2\beta + \frac{2\lambda^2 \cos^2 \theta_W}{g_2^2} \sin^2 2\beta \right) \quad (3)$$

It approaches to the MSSM relation $m_{S_1}^2 < m_Z^2$ for $\tan \beta \rightarrow \infty$ or $\lambda \rightarrow 0$.

The above relation may be cast into a simple form, by noticing that the coefficient of λ above, $2 \cos^2 \theta_W / g_2^2$, is very close to the neutrino- Z coupling constant $g_{\nu\nu Z} = g_2 / 2 \cos \theta_W$. Thus, denoting $\lambda_0 = g_2 / \sqrt{2} \cos \theta_W = \sqrt{2} g_{\nu\nu Z}$, one has $\lambda_0(m_Z) = 0.52$ for $g_{\nu\nu Z}(m_Z) = 0.3714$. With this value, the upper bounds on the S_1 mass at tree level is: $m_{S_1} \leq m_Z$ for $\lambda \leq \lambda_0 = 0.52$ and $m_{S_1} \leq \frac{\lambda}{\lambda_0} m_Z = 1.92 \lambda m_Z$ for $\lambda > \lambda_0$ [8].

The dependence of m_{S_1} on λ comes from the fact that there is a quartic term with the coupling constant λ in the NMSSM. It turns out that the upper bound on λ may be relevant for m_{S_1} . An effective way of determining the upper bound on λ is the renormalization group (RG) equation analysis [9,10].

The 1-loop RG equations involving λ read as

$$\frac{d\lambda}{dt} = \frac{1}{8\pi^2} (k^2 + 2\lambda^2 + \frac{3}{2}h_t^2 - \frac{3}{2}g_2^2 - \frac{1}{2}g_1^2)\lambda$$

$$\begin{aligned}
\frac{dk}{dt} &= \frac{3}{8\pi^2}(k^2 + \lambda^2)k \\
\frac{dh_t}{dt} &= \frac{1}{8\pi^2}\left(\frac{1}{2}\lambda^2 + 3h_t^2 - \frac{8}{3}g_3^2 - \frac{3}{2}g_2^2 - \frac{13}{18}g_1^2\right)h_t \\
\frac{dg_1}{dt} &= \frac{11}{16\pi^2}g_1^3 \\
\frac{dg_2}{dt} &= \frac{1}{16\pi^2}g_2^3 \\
\frac{dg_3}{dt} &= -\frac{3}{16\pi^2}g_3^3
\end{aligned} \tag{4}$$

where $t = \ln \mu$, μ being here the renormalization scale. Numerical integration of the above RG equations by demanding the existence of no Landau poles up to the GUT scale yield the upper bound of λ at the electroweak scale. We plot λ_{\max} as function of $\tan \beta$ for some values of k , for $m_t = 175$ GeV in Fig. 1 and for $m_t = 190$ GeV in Fig. 2.

We find that $0.64 \leq \lambda_{\max} \leq 0.74$ for $175 \leq m_t$ (GeV) ≤ 190 . The upper bound on λ is roughly independent of $\tan \beta$ for $\tan \beta \geq 3$. Also, the two figures show that λ_{\max} decreases with increasing k . The upper bound on k is about 0.7. Moreover, the lower bound on $\tan \beta$ is set at the electroweak scale. We have $\tan \beta \geq 1.24$ for $m_t = 175$ GeV and $\tan \beta \geq 2.6$ for $m_t = 190$ GeV.

Using $0.64 \leq \lambda_{\max} \leq 0.74$, we obtain the tree-level upper bound on m_{S_1} as

$$113 \leq m_{S_1}^{\max} \text{ (GeV)} \leq 131 \tag{5}$$

Our results may well be compared with previous analyses. For example, the upper limit of λ has been estimated to be about 0.87 [9] for $h_t \geq 0.5$, where h_t is the top Yukawa coupling, which yields $m_{S_1} \leq 151$ GeV. By similar analysis of RG equations, the upper limit of λ was obtained as function of h_t , thus yielding an upper bound on m_{S_1} as 140 GeV [10].

However, the above tree-level upper bound does not contain radiative corrections to the mass matrices of Higgs bosons. As in the case of the MSSM, the contributions from the radiative corrections is found to change the tree-level upper bound considerably. Several groups have calculated the higher-order contributions to the mass matrices of Higgs bosons and determined the corrected upper bound on m_{S_1} [8,11,12].

We employ the effective potential method of Coleman and Weinberg [13] to evaluate the higher-order contributions at the 1-loop level. The 1-loop effective potential can then be written as [11]

$$V_1(Q) = V_0(Q) + \Delta V_1(Q) \tag{6}$$

where $V_0(Q)$ is the tree-level potential evaluated with couplings renormalized at the scale Q , and

$$\Delta V_1(Q) = \frac{1}{64\pi^2} \text{STr } \mathcal{M}^4 \left(\ln \frac{\mathcal{M}^2}{Q^2} - \frac{3}{2} \right) \quad (7)$$

is the 1-loop contribution. Here, \mathcal{M}^2 is the field-dependent generalized mass matrix containing mass terms for all the particles in the NMSSM.

The mass matrix M^S of the scalar Higgs bosons at 1-loop level is, to a good approximation [11], given by the second derivative of $V_1(Q)$ with respect to the Higgs fields. Taking only top quark and stop quark contributions into account, and assuming the degeneracy of the left and the right stop quark mass, we find that the higher-order contributions change the relevant elements of the tree-level mass matrix as [8]

$$\begin{aligned} M_{11}^S &\rightarrow M_{11}^S + D_{11} \\ M_{12}^S &\rightarrow M_{12}^S + D_{12} \\ M_{22}^S &\rightarrow M_{22}^S + D_{22} \end{aligned} \quad (8)$$

where

$$\begin{aligned} D_{11} &= -\frac{1}{16\pi^2} \left(\frac{\lambda x A_T}{v_2} \right)^2 \left(\frac{m_t}{m_{\tilde{t}}} \right)^4 \\ D_{12} &= \frac{3}{8\pi^2} \lambda x A_T \left(\frac{m_t^2}{m_{\tilde{t}} v_2} \right)^2 \left(1 + \frac{1}{6} \frac{A_t A_T}{m_{\tilde{t}}^2} \right) \\ D_{22} &= \frac{3}{8\pi^2} \left(\frac{m_t^2}{v_2} \right)^2 \left[2 \ln \left(\frac{m_{\tilde{t}}}{m_t} \right)^2 - \frac{2 A_t A_T}{m_{\tilde{t}}^2} - \frac{1}{6} \frac{A_t^2 A_T^2}{M_t^4} \right] \end{aligned} \quad (9)$$

with $A_T = -A_t + \lambda x \cot \beta$. The b -quark contributions are not included as they are negligibly smaller than the t -quark contributions. Those higher-order contributions render the upper bound on m_{S_1} as

$$(m_{S_1}^{\max})^2 \rightarrow (m_{S_1}^{\max, 1\text{-loop}})^2 = (m_{S_1}^{\max})^2 + D_{11} \cos^2 \beta + D_{12} \sin 2\beta + D_{22} \sin^2 \beta \quad (10)$$

Incorporating the upper bound of the parameter λ from the RGE analysis, we determine the upper bound on m_{S_1} in the parameter regions of the NMSSM for $250 \leq x$ (GeV) ≤ 1000 , $250 \leq A_t$ (GeV) ≤ 1000 , and $250 \leq m_{\tilde{t}}$ (GeV) ≤ 1000 , where x , A_t , and $m_{\tilde{t}}$ are respectively the vev of the Higgs singlet, the soft breaking coefficient of top sector, and stop quark mass, and for $2 \leq \tan \beta \leq 20$, for $175 \leq m_t$ (GeV) ≤ 190 . Our result is:

$$120 \leq m_{S_1}^{\max, 1\text{-loop}} \text{ (GeV)} \leq 156 \quad (11)$$

for the lightest scalar Higgs boson in the NMSSM at the 1-loop level [8].

Also, in terms of $m_{S_1}^{\max}$, it can be shown that the upper bounds on m_{S_2} and m_{S_3} are given as

$$\begin{aligned} m_{S_2}^2 &\leq (m_{S_2}^{\max})^2 = \frac{(m_{S_1}^{\max})^2 - R_1^2 m_{S_1}^2}{1 - R_1^2} \\ m_{S_3}^2 &\leq (m_{S_3}^{\max})^2 = \frac{(m_{S_1}^{\max})^2 - (R_1^2 + R_2^2) m_{S_1}^2}{1 - (R_1^2 + R_2^2)} \end{aligned}$$

where $R_1 = U_{11} \cos \beta + U_{12} \sin \beta$ and $R_2 = U_{21} \cos \beta + U_{22} \sin \beta$, U_{ij} being the 3×3 orthogonal matrix which diagonalizes the mass matrix M^S of the scalar Higgs bosons. Clearly, R_1 and R_2 are complicated functions of the relevant parameters of the NMSSM. Note moreover that they satisfy the unitarity condition $0 \leq R_1^2 + R_2^2 \leq 1$.

That the upper bound on m_{S_1} in the NMSSM at 1-loop level is between 120 and 156 GeV suggests that the accessible region of the parameter space at LEP 1 with $\sqrt{s} = m_Z$ might be very small. Actually, we have shown that the existing LEP 1 data do not exclude the existence of S_1 with $m_{S_1} = 0$ GeV [6].

For the future colliders with $\sqrt{s} = 500, 1000$, or 2000 GeV, the situation is quite different. In this case, the production of the lightest scalar Higgs boson via the Higgsstrahlung process, $e^+e^- \rightarrow S_1 Z$ where Z decays further into a pair of fermion and antifermion, with real Z and real S_1 , is always possible, because the collider energy \sqrt{s} is much larger than $E_T = m_Z + m_{S_1}$:

$$212 \leq E_T^{\max} = m_Z + m_{S_1}^{\max} \text{ (GeV)} \leq 248$$

Thus, E_T plays a kind of threshold energy and is an important quantity of our model. To obtain informations about how far the model could be tested, then, it would be helpful to derive a lower bound on the production cross section of the Higgsstrahlung process, which can be expressed as a function of the collider energy only.

At the proposed center of mass energies of 500, 1000, or 2000 GeV for the future e^+e^- linear colliders, the question is therefore not whether it is kinematically possible to produce S_1 but whether the production rate is large enough for S_1 to be detected. If the production rate of S_1 be small, one should then examine as a next step if that of S_2 or S_3 is large enough. In order to be systematic, we consider all of the productions of S_1 , S_2 , and S_3 via the Higgsstrahlung process.

The cross sections for the productions of the three scalar Higgs bosons via the Higgsstrahlung process can be expressed as

$$\begin{aligned} \sigma_1(R_1, R_2, m_{S_1}) &= \sigma_{SM}(m_{S_1}) R_1^2 \\ \sigma_2(R_1, R_2, m_{S_2}) &= \sigma_{SM}(m_{S_2}) R_2^2 \\ \sigma_3(R_1, R_2, m_{S_3}) &= \sigma_{SM}(m_{S_3})(1 - R_1^2 - R_2^2) \end{aligned} \tag{12}$$

where $\sigma_{SM}(m)$ is the cross section in the standard model for the production of the Higgs boson of mass m via the Higgsstrahlung process. Note that the production cross sections are also functions of \sqrt{s} of the collider, though not explicitly shown. A useful observation is that $\sigma_i(m_{S_i}^{\max}) \leq \sigma_i(m_{S_i})$ which allows one to derive the parameter-independent lower bound on σ_i , as we will see shortly.

Now, we calculate for given R_1 and R_2 the cross section $\sigma_1(R_1, R_2, m_{S_1})$ for S_1 production via the Higgsstrahlung process. We repeat the calculations for S_2 and S_3 productions to obtain $\sigma_2(R_1, R_2, m_{S_2})$ and $\sigma_3(R_1, R_2, m_{S_3})$. Because the production cross sections decrease as the produced Higgs boson mass increases, one has

$$\begin{aligned}\sigma_2(R_1, R_2, m_{S_2}) &\geq \sigma_2(R_1, R_2, m_{S_2}^{\max}) \\ \sigma_3(R_1, R_2, m_{S_3}) &\geq \sigma_3(R_1, R_2, m_{S_3}^{\max})\end{aligned}\tag{13}$$

The second step is to calculate, by allowing m_{S_1} to vary from its minimum to its maximum value, for given R_1 and R_2 , the set of the three production cross sections $\sigma_1(R_1, R_2, m_{S_1})$, $\sigma_2(R_1, R_2, m_{S_2}^{\max})$, and $\sigma_3(R_1, R_2, m_{S_3}^{\max})$. Recall that both $m_{S_2}^{\max}$ and $m_{S_3}^{\max}$ are functions of m_{S_1} .

It is quite clear that each of the three production cross sections will exhibit its own minimum (and maximum) for a certain value of m_{S_1} in the range between its lower and upper bound. Naturally, $\sigma_1(R_1, R_2, m_{S_1})$ is minimized when m_{S_1} is maximized. That is, the minimum of $\sigma_1(R_1, R_2, m_{S_1})$ is given by $\sigma_1(R_1, R_2, m_{S_1}^{\max})$. Let us denote it by $\sigma_1^{\min}(R_1, R_2)$.

For $\sigma_2(R_1, R_2, m_{S_2}^{\max})$ and $\sigma_3(R_1, R_2, m_{S_3}^{\max})$, it is not straightforward to tell where their minima occur within the allowed range of m_{S_1} , because both $m_{S_2}^{\max}$ and $m_{S_3}^{\max}$ are dependent not only on m_{S_1} but also R_1 and R_2 . Nonetheless, the minima of $\sigma_2(R_1, R_2, m_{S_2}^{\max})$ and $\sigma_3(R_1, R_2, m_{S_3}^{\max})$ would exist for certain values of m_{S_1} . Let them be denoted by $\sigma_2^{\min}(R_1, R_2)$ and $\sigma_3^{\min}(R_1, R_2)$, respectively. (Note that the value of m_{S_1} that yields $\sigma_2^{\min}(R_1, R_2)$ is generally different from the one that does $\sigma_3^{\min}(R_1, R_2)$, for given R_1 and R_2 .)

Then, by comparing the three minima with each other, we can establish

$$\sigma(R_1, R_2) = \max\{\sigma_1^{\min}(R_1, R_2), \sigma_2^{\min}(R_1, R_2), \sigma_3^{\min}(R_1, R_2)\}\tag{14}$$

for given R_1 and R_2 . In other words,

$$\sigma_i(R_1, R_2, m_{S_i}) \geq \sigma_i(R_1, R_2, m_{S_i}^{\max}) \geq \sigma_i^{\min}(R_1, R_2, m_{S_i}) = \sigma(R_1, R_2)$$

for some i . The meaning of $\sigma(R_1, R_2)$ cannot be missed: At least one of the three scalar Higgs bosons has its production cross section via the Higgsstrahlung process in e^+e^- collisions larger than $\sigma(R_1, R_2)$ for a certain set of relevant parameters of the NMSSM.

The third step is to plot $\sigma(R_1, R_2)$ in the (R_1, R_2) -plane for given \sqrt{s} . The triangular area in the plane defined by $0 \leq R_1^2 \leq 1$, $0 \leq R_2^2 \leq 1$, and $0 \leq (1 - R_1^2 - R_2^2) \leq 1$ represents the whole space of the relevant parameters of the NMSSM, because it is the entire physical area in the (R_1, R_2) -plane.

We find that $\sigma(R_1, R_2)$ vanishes for the collider energy \sqrt{s} less than $E_T = m_{S_1}^{\max} + m_Z$. This is the case for LEP II with $\sqrt{s} \leq 205$ GeV, which implies that even the highest proposed energy of LEP II would most probably not be able to test our model completely. If \sqrt{s} is larger than E_T , then $\sigma(R_1, R_2)$ never vanishes for that collider energy. Thus, for given $\sqrt{s} \geq E_T$, $\sigma(R_1, R_2)$ exhibits a nonzero minimum somewhere in the (R_1, R_2) -plane.

The final step is to establish the minimum of $\sigma(R_1, R_2)$ in the (R_1, R_2) -plane for given \sqrt{s} . Let it be denoted as $\sigma_0(\sqrt{s})$. Thus, we have

$$\sigma(R_1, R_2) \geq \sigma_0(\sqrt{s})$$

This minimum is a universal minimum in the sense that it is independent of the parameters of the NMSSM. It is the absolute lower bound on at least one of $\sigma_i(R_1, R_2, m_{S_i}) \geq \sigma_0(\sqrt{s})$ for some i : At least one of the three scalar Higgs bosons may be produced via the Higgsstrahlung process in e^+e^- collisions with production cross section larger than $\sigma_0(\sqrt{s})$. This minimum is therefore a characteristic quantity of the NMSSM.

Let us now plot $\sigma(R_1, R_2)$ in the (R_1, R_2) -plane for given \sqrt{s} in order to evaluate $\sigma_0(\sqrt{s})$, its minimum. For simplicity, we set $m_{S_1}^{\max} = 145$ GeV. The dependence of $\sigma(R_1, R_2)$, and hence $\sigma_0(\sqrt{s})$, on $m_{S_1}^{\max}$ is quite small for $\sqrt{s} \geq 500$ GeV, as will be shown shortly.

In Fig. 3, we plot $\sigma(R_1, R_2)$ for $\sqrt{s} = 500$ GeV. The minimum is found to be about 16 fb. When the discovery limit is about 30 events, one would need a luminosity of about 25 fb for the future e^+e^- collider, which is a realistic one. In Fig. 4 and Fig. 5, we repeat our plottings for $\sqrt{s} = 1000$ GeV and 2000 GeV, respectively. We find that the minimum of the production cross section is 4 fb for $\sqrt{s} = 1000$ GeV and 1 fb for 2000 GeV.

To see the dependence of $\sigma_0(\sqrt{s})$ on the collider energy, we plot it as a function of \sqrt{s} in Fig. 6 for some values of $m_{S_1}^{\max}$. It is observed that $\sigma_0(\sqrt{s})$ becomes largest for around $\sqrt{s} = 300$ GeV. Moreover, the effect of $m_{S_1}^{\max}$ is most dominant there. For $\sqrt{s} \geq 500$ GeV, $\sigma_0(\sqrt{s})$ decreases as \sqrt{s} increases. Also, the effect of $m_{S_1}^{\max}$ on $\sigma_0(\sqrt{s})$ becomes rather small there.

As an illustration, the individual production cross sections $\sigma_i(R_1, R_2, m_{S_i})$ are calculated for an exemplary set of the relevant parameters of the NMSSM. Here, not only the Higgsstrahlung process $e^+e^- \rightarrow S_i Z \rightarrow S_i b\bar{b}$ but also the contributions from two other important processes are considered. The two other

processes are the process $e^+e^- \rightarrow Z \rightarrow b\bar{b} \rightarrow S_i b\bar{b}$ where S_i is radiated off from b or \bar{b} , and the process $e^+e^- \rightarrow Z \rightarrow S_i P_j \rightarrow S_i b\bar{b}$ where P_j ($j = 1, 2$) is a pseudoscalar Higgs boson.

The results are plotted in Fig. 7 and Fig. 8, as functions of the collider energy \sqrt{s} , for $A_\lambda = 220$ GeV, $A_k = 160$ GeV, $x = 1000$ GeV, $\lambda = 0.12$, $k = 0.04$, and $\tan\beta = 2$. The production cross sections in Fig. 7 are the tree-level ones, whereas those in Fig. 8 are those with the 1-loop corrections via the effective potential. The relevant parameters for the 1-loop corrections are taken as $A_t = 0$, $m_{\tilde{t}} = 1000$ GeV, and $m_t = 175$ GeV.

For this exemplary set of parameters, the 1-loop corrections is seen to be important for the collider energy of about 150 GeV and decreases as the collider energy increases. Also, for $\sqrt{s} = 500$ GeV and beyond, we find that S_2 would most dominantly be produced for the exemplary set of parameters, both at the tree level and the 1-loop level.

The possibility of detecting one of the three scalar Higgs bosons in the NMSSM at the future e^+e^- linear collider has been analyzed by examining their productions via the Higgsstrahlung process. The whole space of the relevant parameters of the NMSSM is conveniently represented by a triangular area in the (R_1, R_2) -plane, where the production cross sections of the three scalar Higgs bosons in e^+e^- collisions are evaluated for given c.m. energy of the e^+e^- collider.

For the three production cross sections, we have searched their minima in the (R_1, R_2) -plane. Then, from the three minima of the production cross sections, we have established a characteristic quantity for them, $\sigma_0(\sqrt{s})$, which is a kind of universal minimum of the production cross section. Actually, it is the largest one among the three minima of the production cross sections. We have obtained that $\sigma_0(\sqrt{s}) = 16$ fb, 4 fb, and 1 fb for $\sqrt{s} = 500$ GeV, 1000 GeV, and 2000 GeV, respectively. As stressed in the preceding section, these numbers indicate that at least one of the three scalar Higgs bosons may be produced via the Higgsstrahlung process in e^+e^- collisions with production cross section larger than $\sigma_0(\sqrt{s})$.

What we have found indicate that, for a certain set or regions of the relevant parameters of the NMSSM, at least one of the three scalar Higgs bosons might have a reasonable mass and a reasonable production cross sections such that it might be produced at the future e^+e^- colliders. We conclude that the Higgs sector of the NMSSM can most probably be tested at the future linear e^+e^- colliders with $\sqrt{s} = 500, 1000, \text{ or } 2000$ GeV.

After we completed this article, we have been informed that a similar conclusion has been drawn by Gunion, Haber, and Moroi [14]. However, their approach is quite different from ours.

This work is supported in part by the joint program between DFG and KOSEF and in part by the Basic Science Research Institute Program, Ministry of Education, BSRI-97-2442 (Korea).

References

- [1] J. F. Gunion, H. E. Haber, G. L. Kane, and S. Dawson, *The Higgs Hunters' Guide* (Addison-Wesley Pub. Co., Redwood City, CA, USA, 1990).
- [2] H. E. Haber and G. L. Kane, **Phys. Rep.** **117** (1985) 75.
- [3] H. P. Nilles, **Phys. Rep.** **110** (1984) 1.
- [4] B. R. Kim, S. K. Oh, and A. Stephan, in *Proc. Workshop on Physics and Experiment with Linear e^+e^- Colliders*, eds. F. A. Harris *et al.* (World Scientific, Singapore, 1993) 860.
- [5] F. Richard, in *Proc. 27th Int. Conf. on High Energy Phys.*, eds. P. J. Bussy and I. G. Knowles (IOP Pub., Bristol, 1994) 779;
M. Pieri, *ibid.*, 783.
- [6] B. R. Kim, S. K. Oh, A. Stephan, in *e^+e^- Collisions at 500 GeV: The Physics Potential*, DESY 92-123B (1992) 697; DESY 93-123C (1993) 491; Aachen preprint, PITHA 93/36 (1993).
- [7] B. R. Kim, G. Kreyerhoff, and S. K. Oh, in *e^+e^- Collisions at TeV Energies: The Physics Potential*, DESY 96-123D (1996) 213.
- [8] B. R. Kim and S. K. Oh, Aachen preprint, PITHA 94/46 (1994).
- [9] J. Ellis, J. F. Gunion, H. E. Haber, L. Roszkowski, F. Zwirner, **Phys. Rev. D** **39** (1989) 844;
M. Drees, **Int. J. Mod. Phys. A** **4** (1989) 3635;
J. P. Derendinger and C. A. Savoy, **Nucl. Phys. B** **237** (1984) 307;
S. W. Ham, S. K. Oh, and B. R. Kim, **J. Phys. G: Nucl. Part. Phys.** **22** (1996) 1575.
- [10] J. R. Espinosa and M. Quiros, **Phys. Lett. B** **279** (1992) 92;
U. Ellwanger and M. Lindner, Heidelberg preprint, HD-THEP-92-48 (1992);
P. Binetrui and C. A. Savoy, **Phys. Lett. B** **277** (1992) 453;
K. Inoue, A. Kakuto, H. Komatsu, S. Takeshita, **Prog. Theor. Phys.** **68** (1982) 927.
- [11] J. Ellis, G. Ridolfi, F. Zwirner, **Phys. Lett. B** **257** (1991) 83; **Phys. Lett. B** **262** (1991) 477.
- [12] P. N. Pandita, **Z. Phys. C** **59** (1993) 575;
U. Ellwanger, **Phys. Lett. B** **303** (1993) 271;
T. Elliott, S. F. King, and P. L. White, **Phys. Rev. D** **49** (1994) 2435.
- [13] S. Coleman and E. Weinberg, **Phys. Rev. D** **7** (1973) 1888.
- [14] J. F. Gunion, H. E. Haber, and T. Moroi, UCD Preprint, UCD-96-26 (1996).

Figure Captions

Figure 1: The upper bound on λ as function of $\tan\beta$ for some values of k , for $m_t = 175$ GeV.

Figure 2: The upper bound on λ as function of $\tan\beta$ for some values of k , for $m_t = 190$ GeV.

Figure 3: The contours of $\sigma(R_1, R_2)$ in the (R_1, R_2) -plane for $m_{S_1}^{\max} = 145$ GeV and $\sqrt{s} = 500$ GeV.

Figure 4: The contours of $\sigma(R_1, R_2)$ in the (R_1, R_2) -plane for $m_{S_1}^{\max} = 145$ GeV and $\sqrt{s} = 1000$ GeV.

Figure 5: The contours of $\sigma(R_1, R_2)$ in the (R_1, R_2) -plane for $m_{S_1}^{\max} = 145$ GeV and $\sqrt{s} = 2000$ GeV.

Figure 6: $\sigma_0(\sqrt{s})$, the minimum of $\sigma(R_1, R_2)$, as function of the collider energy \sqrt{s} for some values of $m_{S_1}^{\max}$.

Figure 7: The production cross sections at the tree level $\sigma(e^+e^- \rightarrow b\bar{b}S_i)$ ($i = 1, 2, 3$) as function of the collider energy \sqrt{s} , for $A_\lambda = 220$ GeV, $A_k = 160$ GeV, $x = 1000$ GeV, $\lambda = 0.12$, $k = 0.04$, and $\tan\beta = 2$. The solid, dashed, and dashed-dotted curves correspond respectively to the S_1 , S_2 , and S_3 productions.

Figure 8: The production cross sections at the 1-loop level $\sigma(e^+e^- \rightarrow b\bar{b}S_i)$ ($i = 1, 2, 3$) as function of the collider energy \sqrt{s} , for $A_\lambda = 220$ GeV, $A_k = 160$ GeV, $x = 1000$ GeV, $\lambda = 0.12$, $k = 0.04$, and $\tan\beta = 2$. The 1-loop parameters are taken as $A_t = 0$, $m_{\tilde{t}} = 1000$ GeV, and $m_t = 175$ GeV. The solid, dashed, and dashed-dotted curves correspond respectively to the S_1 , S_2 , and S_3 productions.

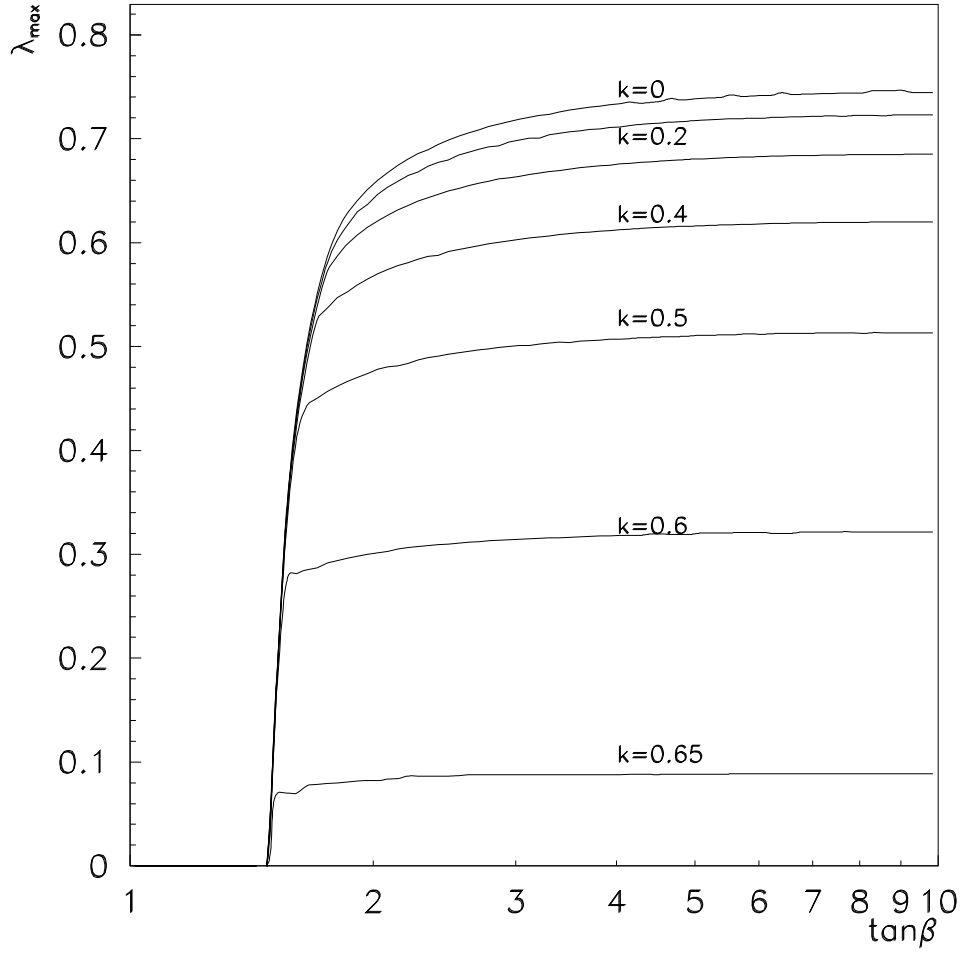


Figure 1: The upper bound on λ as function of $\tan\beta$ for some values of k , for $m_t = 175$ GeV.

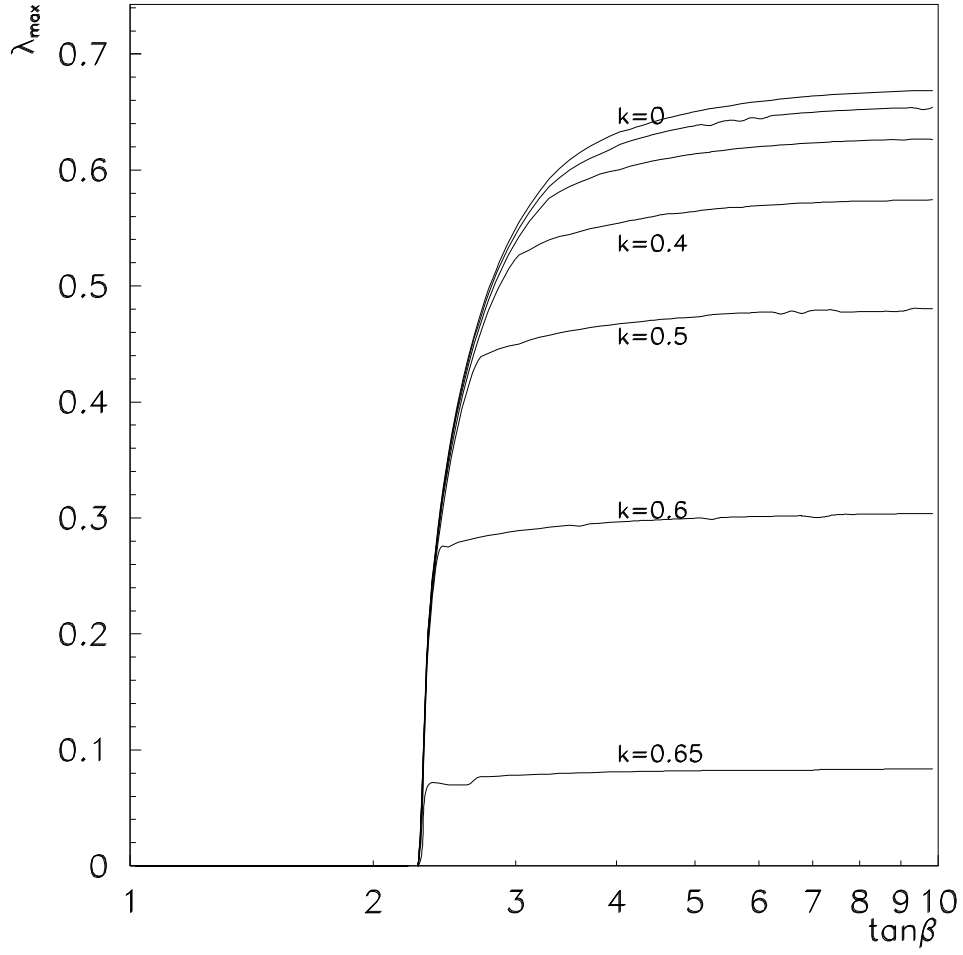


Figure 2: The upper bound on λ as function of $\tan\beta$ for some values of k , for $m_t = 190$ GeV.

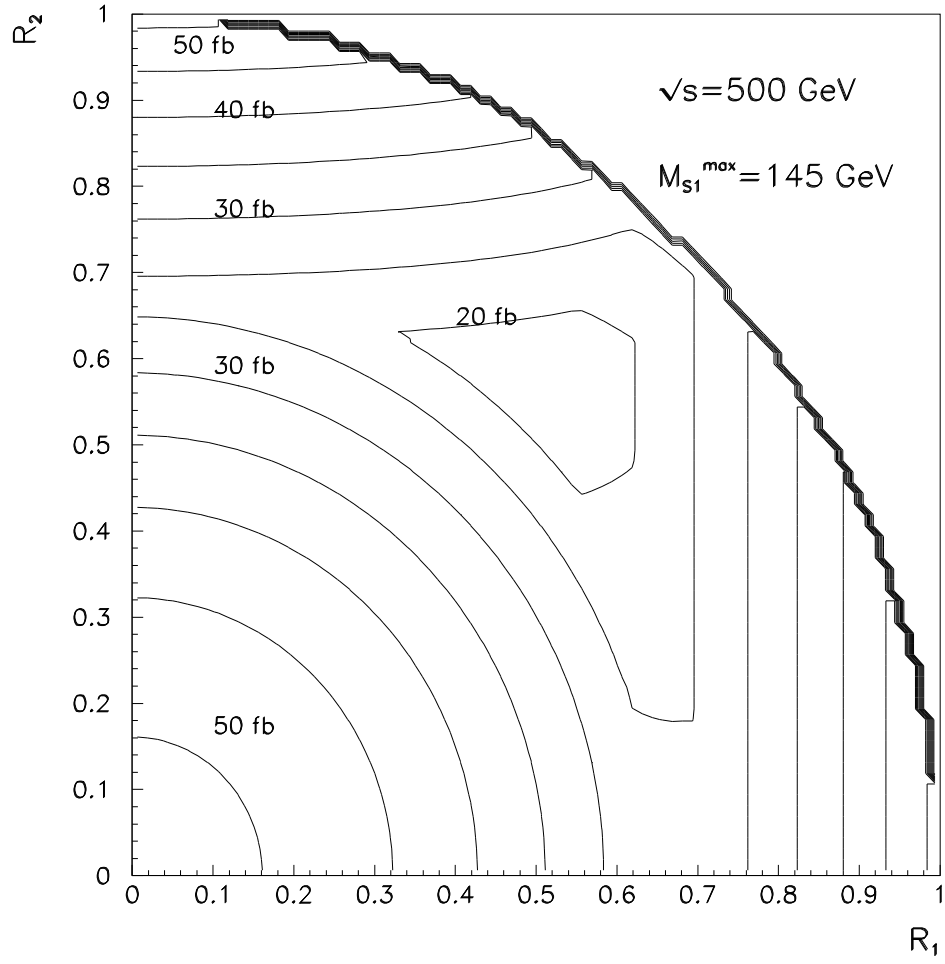


Figure 3: The contours of $\sigma(R_1, R_2)$ in the (R_1, R_2) -plane for $m_{S_1}^{\max} = 145$ GeV and $\sqrt{s} = 500$ GeV.

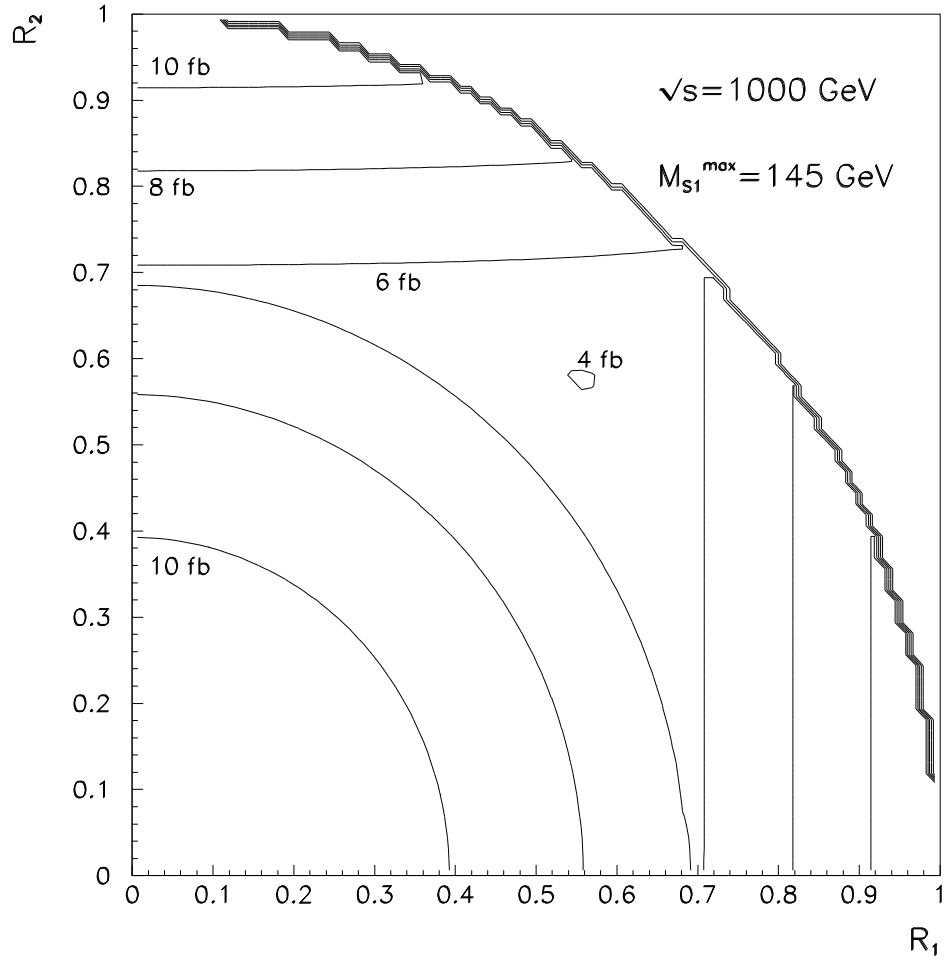


Figure 4: The contours of $\sigma(R_1, R_2)$ in the (R_1, R_2) -plane for $m_{S_1}^{\max} = 145$ GeV and $\sqrt{s} = 1000$ GeV.

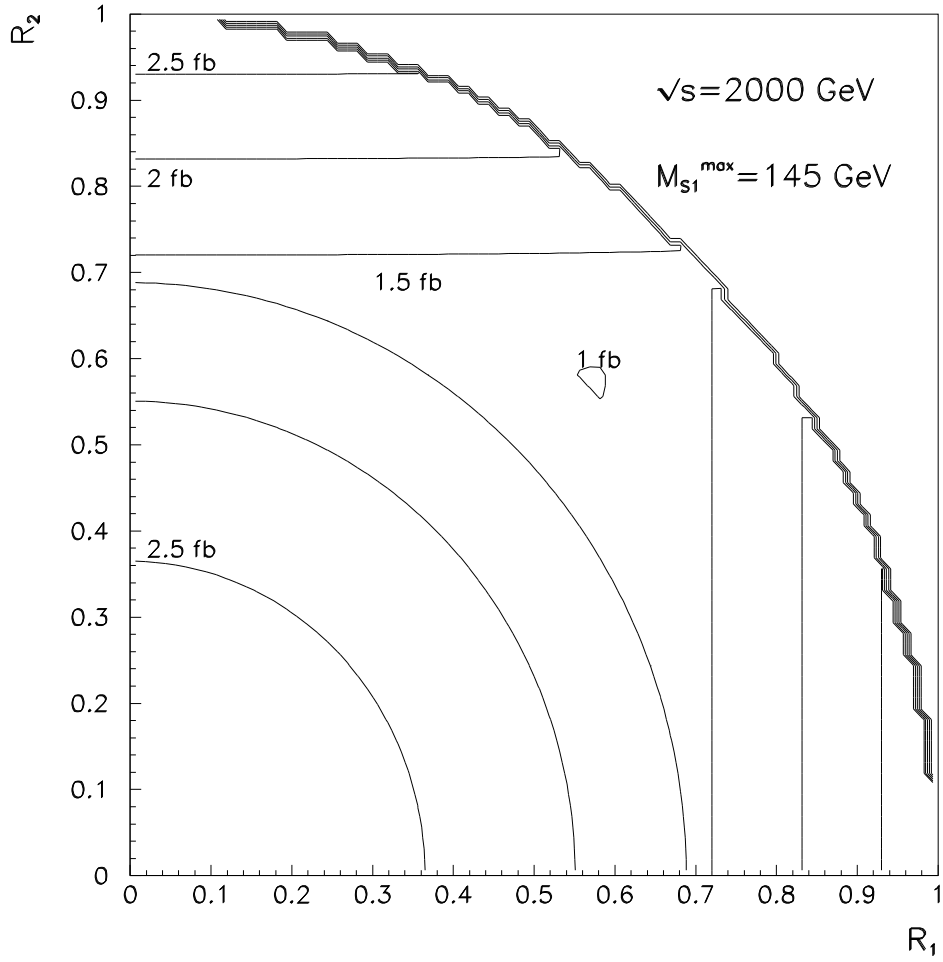


Figure 5: The contours of $\sigma(R_1, R_2)$ in the (R_1, R_2) -plane for $m_{S_1}^{\max} = 145$ GeV and $\sqrt{s} = 2000$ GeV.

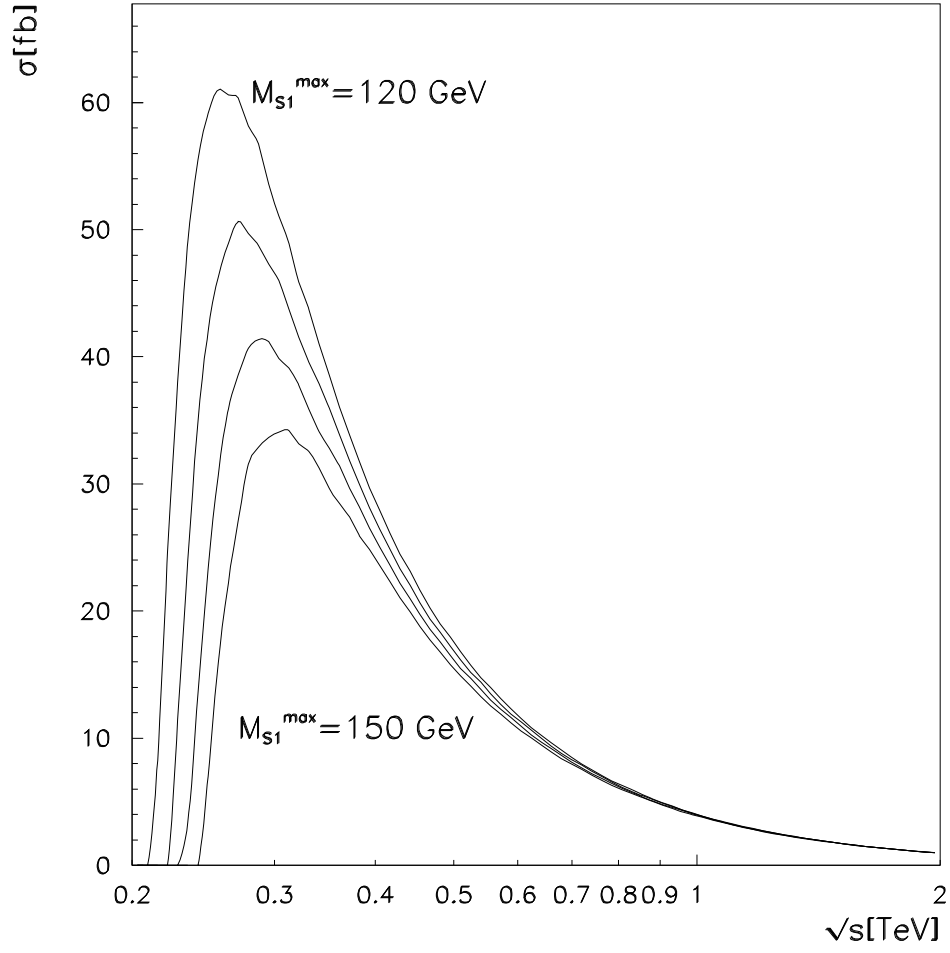


Figure 6: $\sigma_0(\sqrt{s})$, the minimum of $\sigma(R_1, R_2)$, as function of the collider energy \sqrt{s} for some values of $m_{S_1}^{\max}$.

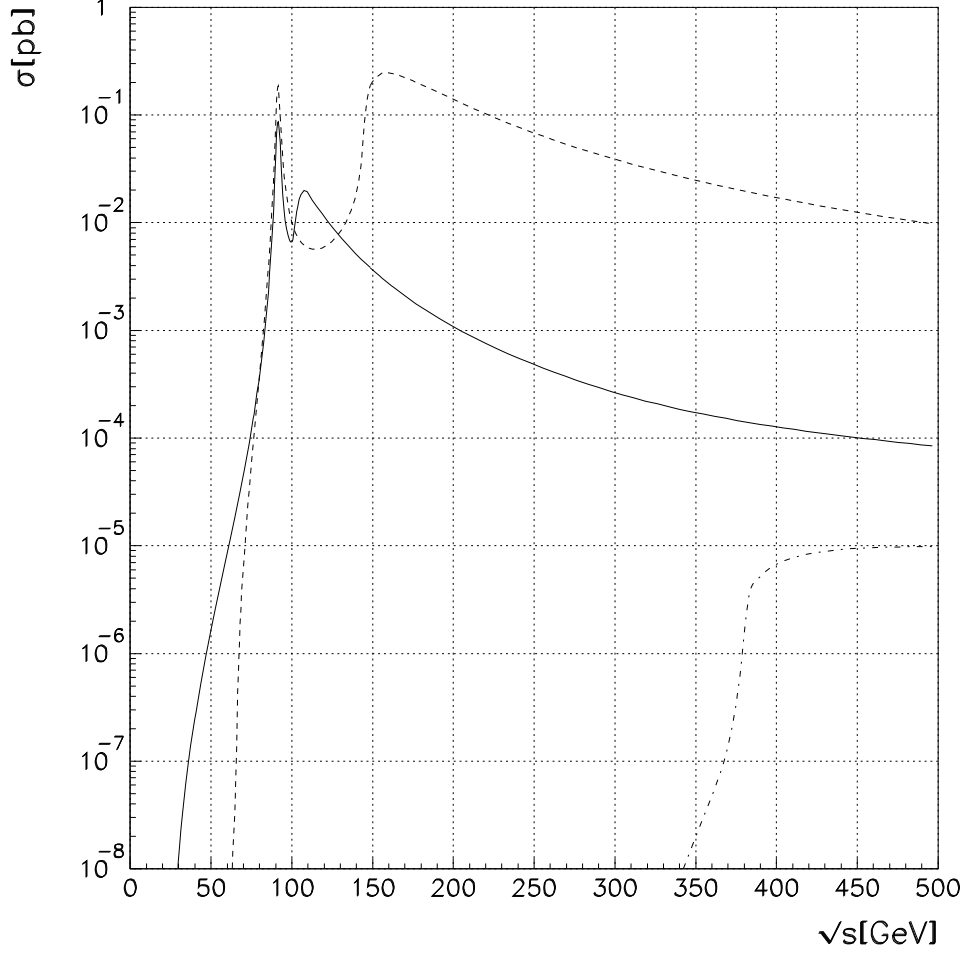


Figure 7: The production cross sections at the tree level $\sigma(e^+e^- \rightarrow b\bar{b}S_i)$ ($i = 1, 2, 3$) as function of the collider energy \sqrt{s} , for $A_\lambda = 220$ GeV, $A_k = 160$ GeV, $x = 1000$ GeV, $\lambda = 0.12$, $k = 0.04$, and $\tan\beta = 2$. The solid, dashed, and dashed-dotted curves correspond respectively to the S_1 , S_2 , and S_3 productions.

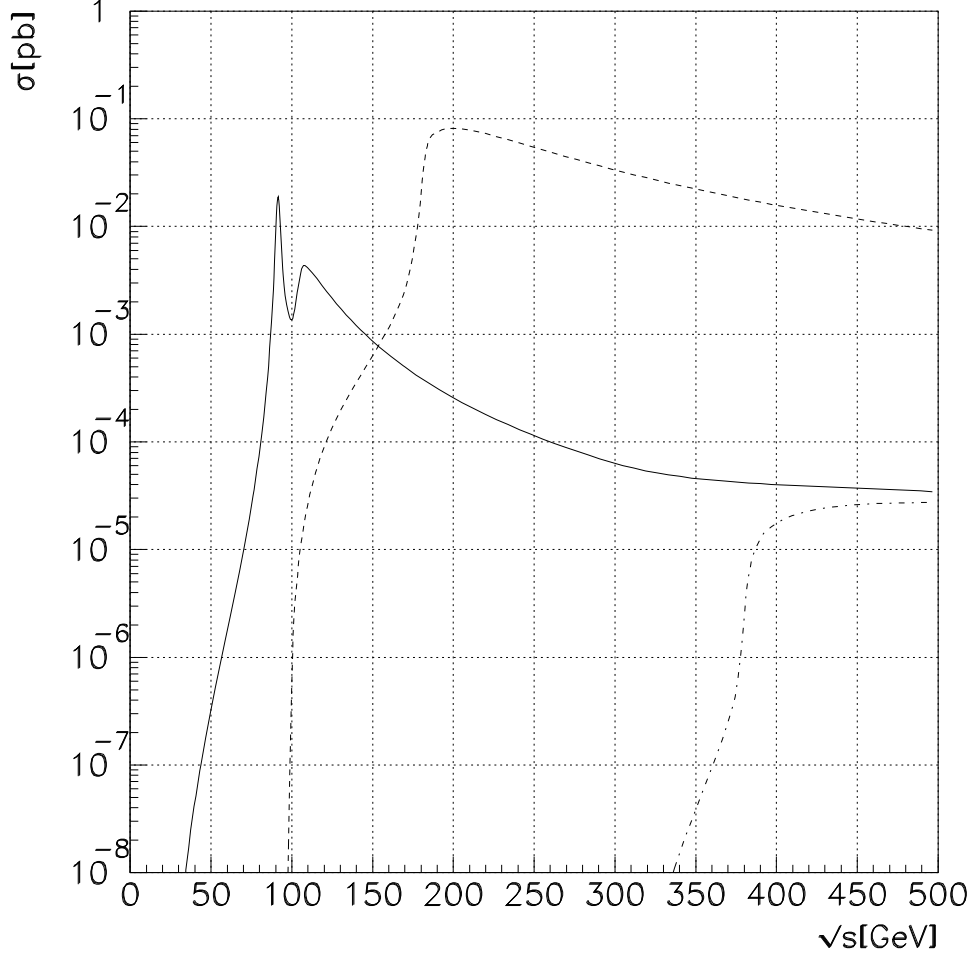


Figure 8: The production cross sections at the 1-loop level $\sigma(e^+e^- \rightarrow b\bar{b}S_i)$ ($i = 1, 2, 3$) as function of the collider energy \sqrt{s} , for $A_\lambda = 220$ GeV, $A_k = 160$ GeV, $x = 1000$ GeV, $\lambda = 0.12$, $k = 0.04$, and $\tan\beta = 2$. The 1-loop parameters are taken as $A_t = 0$, $m_{\tilde{t}} = 1000$ GeV, and $m_t = 175$ GeV. The solid, dashed, and dashed-dotted curves correspond respectively to the S_1 , S_2 , and S_3 productions.